Journal of Alloys and Compounds 509 (2011) 2094–2098

Contents lists available at ScienceDirect

Journal of Alloys and Compounds

journal homepage: www.elsevier.com/locate/jallcom

# Growth of homogenous CuO nano-structured thin films by a simple solution method

F. Bayansal[a,*], S. Kahraman[a], G. Çankaya[b], H.A. Çetinkara[a], H.S. Güder[a], H.M. Çakmak[a]

[a] Physics Department, Mustafa Kemal University, 31034 Hatay, Turkey
[b] Physics Department, Gaziosmanpaşa University, 60250 Tokat, Turkey

ARTICLE INFO

*Article history:*
Received 13 September 2010
Received in revised form 12 October 2010
Accepted 27 October 2010
Available online 4 November 2010

*Keywords:*
CuO
Nanostructure
Solution synthesis
Thin film
Glass substrate
Band gap
Impurity levels

ABSTRACT

This paper describes a simple, low temperature and cost effective solution method to synthesize homogenous cupric oxide (CuO) nano-structured thin films. By this method dense and continuous CuO films with good crystallinity can be prepared in a short time, e.g., in 15 min. The scanning electron microscopy illustrated that the synthesized CuO plate-like nanostructures have RMS thicknesses of 100 nm. The XRD measurements showed that the synthesized CuO nanostructures have a high crystallinity with monoclinic crystal structure preferentially in $(\bar{1}\,1\,1)$ and $(1\,1\,1)$ directions. From the temperature dependant dark electrical resistivity measurements the ionization energies of the impurity levels and thermal band gap energies of the films were calculated.



## 1. Introduction

Since carbon nanotubes were discovered by Iijima [1] in 1991, nanoscaled one-dimensional (1D) and two-dimensional (2D) materials such as nanowires [2–4], nanorods [5,6], nanoribbons [7,8] and nanosheets [9–11] have attracted more attentions due to their unique optical, electrical and magnetic properties and their potential applications in nanodevices [12]. Decreasing the dimensions beneath nano-scale reveals extraordinary and surprising properties of materials. Owing to these novel properties, many researchers work on nano-structured materials in order to use them as building blocks for the integration of the next generation of nanoelectronics, ultra small optical devices, biosensors, etc.

As promising materials, metal oxide nanostructures have attracted much attention because of their extraordinary properties in different fields of optics, optoelectronics, electronics, catalysts, sensors and so on. In this respect cupric oxide (CuO), a p-type semiconductor with a band gap of 1.2 eV, has received much attention for its various application which are in optoelectronics, catalysis, semiconductors, batteries, gas sensors, biosensors and field transistors [13]. One of the important advantages of using CuO in device applications is that it is non-toxic and its constituents are available in abundance [14]. Because the chemical and physical properties of CuO are strictly dependant of its size and morphology, in the past decade considerable efforts have been made to synthesize various CuO nanostructures. A number of different techniques have been used to control the size and morphology of the CuO nanoparticles such as thermal oxidation [4], electrodeposition [15], quick-precipitation [16], hydrothermal treatment [17], high-temperature combustion [8], thermal evaporation [18] and solution synthesis [19]. Among these methods, solution synthesis, hydrothermal and quick-precipitation methods are important for their safety, environment friendly, ease of mass production and cost-effectiveness. By applying these methods there have been reported considerable powders of CuO nanoparticles [20,21]. But nano-structured CuO thin films that were grown on a substrate have been seldom reported. Some of them used Cu foils as substrates [22,23], but only a few of them used some other materials like microscope glasses and stainless steel slices as substrates [24,25]. For this reason there exist necessities on the researches about CuO thin film that are grown on substrates except Cu foils.

In this work we report a simple route for the synthesis of dense, continuous and stable plate-like nanostructured CuO films by immersing glass substrates in an aqueous solution of copper(II) chloride dehydrate and ammonia. We have investigated the growth mechanism and the optimization conditions to synthesize CuO films. Besides, we have investigated the temperature dependent dark electrical resistivity measurements in order to calculate the

* Corresponding author. Tel.: +90 326 2455845; fax: +90 326 2455867.
*E-mail address:* fbayy@hotmail.com (F. Bayansal).

0925-8388/$ – see front matter © 2010 Elsevier B.V. All rights reserved.
doi:10.1016/j.jallcom.2010.10.146

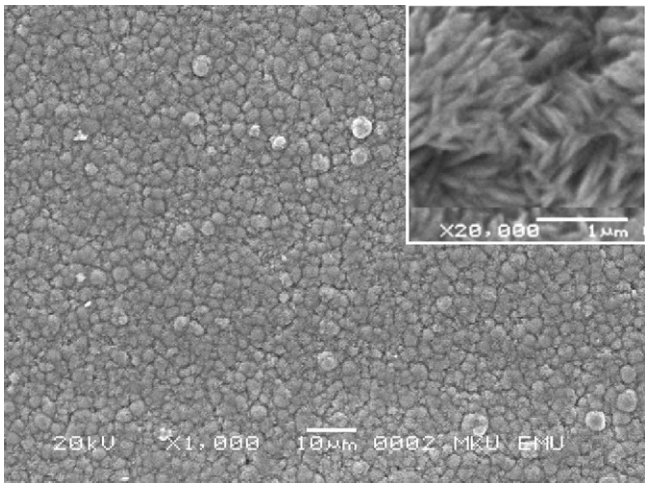


**Fig. 1.** SEM image of the as-synthesized CuO nanoplates. The inset is the high magnification SEM image showing the plate-like structures.

ionization energies of the impurity levels and the band gap energies of synthesized films.

## 2. Experimental details

All the chemical reagents used in the experiment were analytical grade, purchased Sigma–Aldrich Company and Merck KGaA. Cleaning process of the substrates (microscope glass slides) consists of three steps which are cleaning in dilute sulfuric acid solution ($H_2SO_4$:$H_2O$, 1:5, v/v), in acetone and in double distilled water for 5 min each in ultrasonic bath. Synthesis of the films was described as follows: First, 1.705 g copper(II) chloride dehydrate ($CuCl_2{\cdot}2H_2O$) was mixed with 100 $cm^3$ double distilled water (18.2 MΩ $cm^{-2}$) to obtain 0.1 M copper chloride solution. Then the solution was stirred in a magnetic stirrer at room temperature for 1 h in order to get a transparent and well-dissolved solution. After stirring, pH value of the solution was increased to 10.0 by adding aqueous ammonia ($NH_3$). The pH of the solution was measured by Hanna pH 211/213 pH Meter. Previously cleaned substrates were dipped into the solution and the solution was started to boil at about 90 °C. Heating rate was 10 °C/min and it took about 10 min to boil the solution. After 15 min boiling, the substrates were taken out from the bath and rinsed in double distilled water for about 5 min in an ultrasonic bath in order to remove larger and loosely bonded CuO particles. To investigate the effects of heat treatments to the films, four series of samples produced. The first one was kept at room temperature, the second, third and the last samples were annealed at 300 °C for 1, 2 and 3 h respectively in a PROTHERM PTF 12/50/450 tube furnace.

The crystal structure of the samples was examined by Philips X'pert Pro X-ray diffractometer (XRD) (Cu Kα radiation, λ = 1.540056 Å). A JEOL JSM-5500LV scanning electron microscope (SEM) was used for morphological imaging. The film thicknesses were measured by gravimetric calculations and by crossectional SEM analyses. And a Keithley 6487 Picoammeter/Voltage Source was used to investigate the temperature dependant dark resistivity measurements in order to calculate ionization energies of impurity levels and band gap energies of the films.

## 3. Results and discussion

### 3.1. Crystal structure and morphology

The morphology and microstructure of the CuO products were examined by scanning electron microscopy (SEM). Fig. 1 shows the SEM images of as-synthesized CuO films. It can be seen that the substrates are fully covered by clusters of CuO nanoplates. As seen from Fig. 2, the annealing process decreases both the diameters of clusters and thicknesses of nanoplates. Before annealing the cluster diameters are in between 1.6 μm and 4.0 μm (average 2.5 μm) and thickness of the nanoplates are in between 100 nm and 125 nm. After annealing (300 °C for 1 h) the cluster diameters decrease to the values between 1.4 μm and 2.4 μm (average 1.9 μm) and nanoplate thicknesses decrease to the values between 50 nm and 100 nm. Fig. 3 shows the cross-sectional SEM image from which the thicknesses of the films can be measured. Thicknesses of as-synthesized films are in between 2.44 μm and 2.60 μm, on the other hand thicknesses of annealed films changes from 2.20 μm to 2.48 μm. These values are listed in Table 1. From the gravimetric measurements the average film thickness was found as about 1.95 μm for as-synthesized films which implies that the porosity (≈23%) of the films is high. Also the decrease in the thickness of the annealed film that measured by gravimetric method is in convenient with

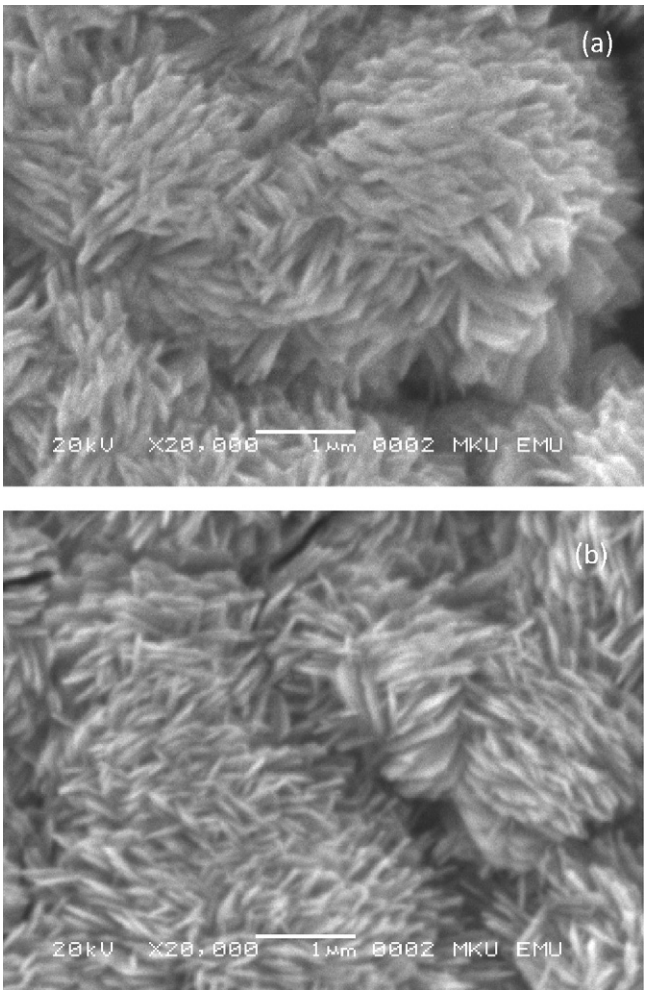


**Fig. 2.** SEM images of the CuO nanoplates (a) as-synthesized; and (b) annealed at 300 °C for 1 h.

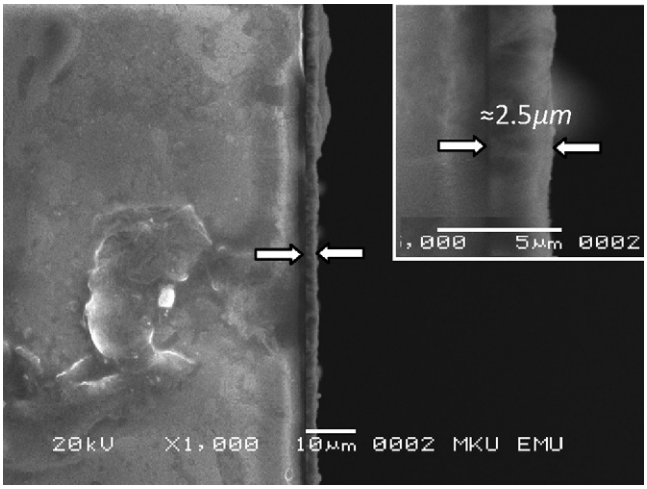


**Fig. 3.** Crossectional SEM image of the as-synthesized CuO film.

**Table 1**
Band gap energies, ionization energies of the impurity levels, cluster diameters, film thicknesses and nano-plate thicknesses of as-synthesized and annealed films (at 300 °C for 1 h).

| | $E_g$ (eV) | $\Delta E$ (eV) | Cluster diameters (μm) | Film thicknesses (μm) | Plate thicknesses (nm) |
|---|---|---|---|---|---|
| As-synthesized | 1.37 | 0.30 | 1.6–4.0 | 2.44–2.66 | 100–125 |
| Annealed at 300 °C for 1 h | 1.39 | 0.32 | 1.4–2.4 | 2.20–2.48 | 50–100 |

that of the crossectional SEM measurements. Heat treatment can cause a re-crystallization and can convert $Cu(OH)_2$ into CuO and $H_2O$, thus re-crystallization or removing water from the structure can cause a decrease or increase (in our experiments a decrease was occurred), that the similar effect has been observed by Shinde et al. [26], in the dimensions of the nanoplates, clusters and in the thickness of the films. In the XRD analysis there was no evidence for the existence of $Cu(OH)_2$. This may be because $Cu(OH)_2$ may be present in small extent (that the signal coming from $Cu(OH)_2$ vanishes in the ground signal) and accumulated along grain boundaries of the crystallites constituting the film or $Cu(OH)_2$ may be amorphous.

XRD analyses were employed to study the crystal structures of the as-synthesized and annealed films. Fig. 4 shows a typical XRD pattern of the films that are as-synthesized and annealed at different temperatures. All diffraction peaks can be clearly indexed to the monoclinic CuO phase with lattice constants of $a = 4.684$ Å, $b = 3.425$ Å, $c = 5.129$ Å, and $\beta = 99.47°$ (JCPDS Card No.: 05-0661). But there was no XRD peaks referred to $Cu(OH)_2$, which means the grown film completely consist of only CuO molecules or $Cu(OH)_2$ may be present in small extent and accumulated along grain boundaries of the crystallites constituting the film. The XRD pattern also provides information on crystal orientations; the Miller-indexed $(\bar{1}\,1\,1)$ and $(1\,1\,1)$ reflections are the strongest, which indicate that they are preferential crystal planes of the nanoplates. From the XRD patterns it can be deduced that annealing causes an increase in the intensities of the peaks $(\bar{1}\,1\,1)$ and $(1\,1\,1)$. Relative intensity values of these orientations change from 38 to 49 and from 37 to 44 respectively. From the SEM images and XRD patterns it was concluded that annealing time made very little effect on the electrical and morphological properties of the films. But, the effects of annealing temperature on the electrical and morphological properties of CuO should be investigated.

### 3.2. Electrical measurements

Silver paste was used to make ohmic contacts with CuO thin films. The current–voltage ($I$–$V$) characteristics of CuO ohmic contacts are presented in Fig. 5. As can be seen, $I$–$V$ dependence is linear within the studied voltage range and this proves that the contact is ohmic. Namely, the derivative $(\partial I/\partial V)^{-1}$ is constant and practically equal to the dark electrical resistance of investigated CuO thin film, indicating a negligible value of the contact resistance [27].

We have measured the temperature dependence (in the range of 300–500 K) of dark electrical resistivity of both as-prepared and annealed CuO thin films in order to determine the ionization energies of the impurity levels and the thermal band gap energies of the films.

As may be shown from the solid-state theory of semiconductors [28,29], in case of a semiconductor with one or more impurity levels, the temperature dependence of dark electrical resistance is given by

$$R(T) = R_0 \exp\left(\frac{E_g}{2kT}\right) + \sum_{i=1}^{n} R'_{0,i} \exp\left(\frac{\Delta E_i}{kT}\right) \quad (1)$$

In previous equation, $R_0$ and $R'_{0,i}$ are constants, $E_g$ is the thermal band gap energy, $\Delta E_i$ is the impurity level ionization energies, $k$ is Boltzmann constant, and $T$ is temperature. In the region of relatively lower temperatures, the overall conductivity of the semiconductor samples is dominated by the charge carriers generated by ionization of impurity levels (extrinsic conductivity), and thus the second term in Eq. (1) prevails in the $R(T)$ dependence. At sufficiently higher temperatures, on the other hand, the temperature dependence of conductivity is dominated by the band-to-band electronic transitions. Under such conditions, the charge carriers acquire enough thermal energy to make an inter-band transition (the intrinsic conductivity is "activated" at these temperatures) [29]. According to previous discussion, the two terms appearing in Eq. (1) may be treated independently in the corresponding temperature intervals. So in the graph of $\ln(R)$ vs $1000/T$ a number of linear trends appear which indicate the forbidden band gap and a number of impurity levels (band gap states) in the forbidden band gap.

As seen in Figs. 6 and 7, there exist only two linear regions. In the higher temperature interval (higher than 470 K), the overall

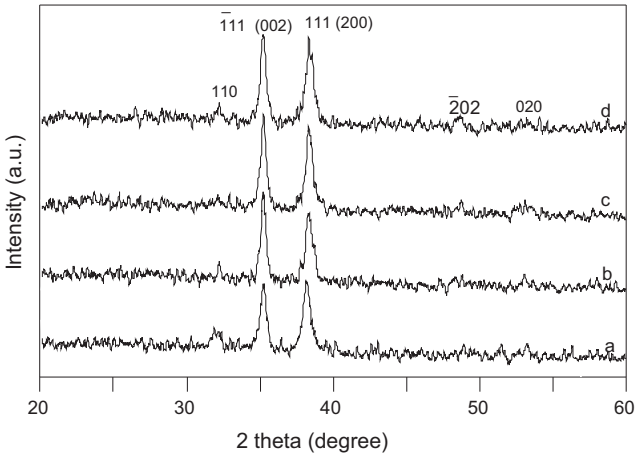


**Fig. 4.** XRD patterns of the CuO films (a) as-synthesized; (b) annealed at 300 °C for 1 h; (c) for 2 h; and (d) for 3 h.

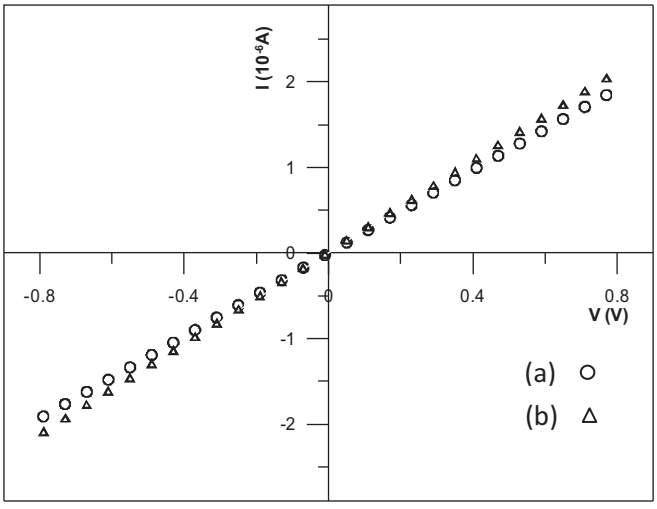


**Fig. 5.** The current–voltage characteristics of CuO thin films (a) as-synthesized; and (b) annealed at 300 °C for 1 h.

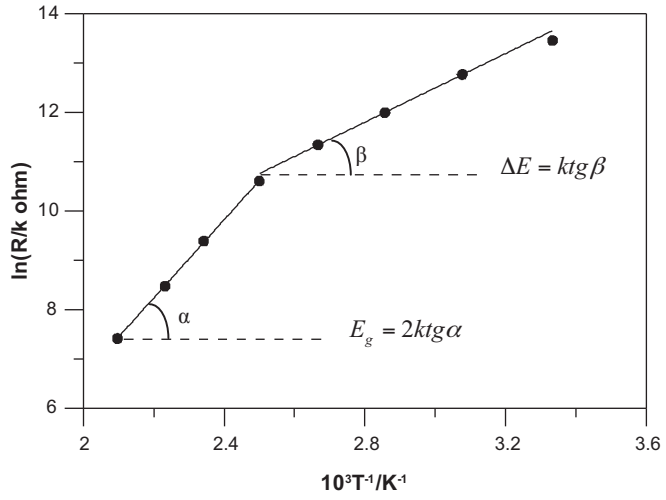


**Fig. 6.** The dependence of ln $R$ vs. $1/T$ for as-synthesized CuO thin film.

$R(T)$ dependence is predominated by the intrinsic charge carriers generation, and is therefore to a good approximation given by

$$R(T) = R_0 \exp\left(\frac{E_g}{2kT}\right) \tag{2}$$

From Eq. (2) $E_g$ can be easily written as

$$E_g = 2k\frac{d\ \ln(R(T))}{d(1/T)} \tag{3}$$

The band gaps were calculated from the slopes of ln($R$) vs. 1000/$T$ graphs. The obtained values for $E_g$ are 1.37 eV and 1.39 eV for as-sythesized and annealed films (at 300 °C for 1 h). These values are in very good agreement with the one obtained from optical spectroscopy measurements [30]. However, exact matching of these two values is not expected, since the optical band gap value refers to room temperature, while the thermal one [28,29] refers to 0 K.

The decrease of dark electrical resistance upon increase of temperature in the region of extrinsic conductivity (corresponding to the lower temperature interval) follows the equation:

$$R(T) = \sum_{i=1}^{n} R'_{0,i} \exp\left(\frac{\Delta E_i}{kT}\right) \tag{4}$$

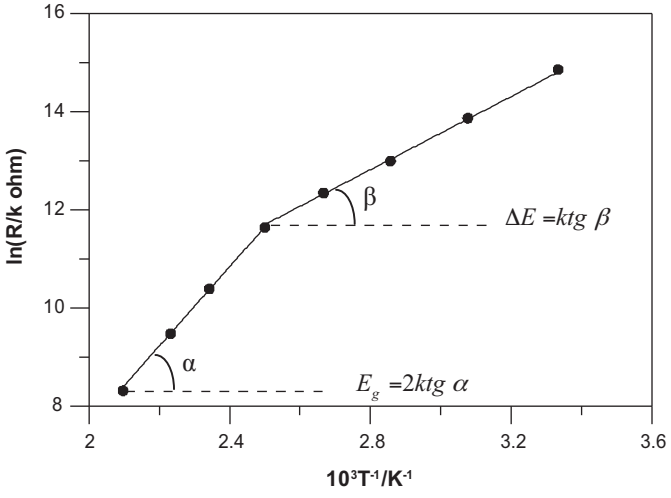


**Fig. 7.** The dependence of ln $R$ vs. $1/T$ for the films annealed at 300 °C for 1 h.

As seen from Figs. 6 and 7, there exists only one impurity level (one linear region at low temperatures). Thus by using Eq. (2) $\Delta E$ can be easily written as

$$\Delta E = k\frac{d\ \ln(R(T))}{d(1/T)} \tag{5}$$

The impurity level ionization energies were calculated from the slopes of ln($R$) vs. 1000/$T$ graphs. The obtained impurity level ionization energy ($\Delta E$) values are 0.30 eV and 0.32 eV for as-sythesized and annealed films (at 300 °C for 1 h). The ionization energies of the impurity levels and the band gap energies of as-synthesized and annealed films are listed in Table 1.

### 3.3. The growth mechanism

For copper ions aqueous solution, when the ion product (*IP*) of the solution is higher than solubility product (*SP*), the precipitation $Cu(OH)_2$ occurs. It is commonly accepted that the degree of supersaturation ($S$), defined as the ratio of *IP* to *SP*, is an important parameter to evaluate the precipitation process in aqueous solution. If $S$ is lower than 1, no precipitation occurs, if $S$ is higher than 1 but lower than a critical value $S_c$, a heterogeneous precipitation occurs on the walls of container and substrate because the value of $S$ is not sufficient to induce nuclei in the bulk solution and if $S$ is higher than $S_c$, a homogenous precipitation occurs in the bulk solution [31]. According to this theory, $S$ value for copper ions must be fixed in between 1 and $S_c$ in order to get heterogeneous nucleation on the substrate.

In this work $CuCl_2{\cdot}2H_2O$ and $NH_3$ were used as ion source and reagent respectively. $Cu^{+2}$ ions were obtained by dissolving 1.705 g $CuCl_2{\cdot}2H_2O$ in double distilled water as shown in Eq. (6). Before the start of precipitation reaction, the pH value of solution was about 3.80. The possible chemical reactions are as follows:

$$CuCl_2{\cdot}2H_2O \rightarrow Cu^{+2}{}_{(aq)} + 2Cl^-{}_{(aq)} \tag{6}$$

$$NH_3 + H_2O \leftrightarrow NH_4{}^+{}_{(aq)} + OH^-{}_{(aq)} \tag{7}$$

$$Cu^{+2}{}_{(aq)} + 2OH^-{}_{(aq)} \rightarrow Cu(OH)_2 \tag{8}$$

$$Cu(OH)_2 \rightarrow CuO + H_2O \tag{9}$$

In the suggested reaction scheme, ammonia played key role for the formation of desired CuO nanostructures. The pH value of the solution is raised to the value of 10.0 by adding ammonia which introduces ammonium and $OH^-$ ions (Eq. (7)). This is the critical stage in the chemical reaction because this stage controls the supply of $OH^-$ ions which determines the degree of supersaturation $S$. And also $Cu(OH)_2$ precipitate cannot dissolve in the solution with a high $OH^-$ concentration to form dissoluble complex ions such as $Cu(OH)_4{}^{-2}$. Therefore we believe that CuO crystalline nuclei in nanoscale were formed in the dehydration of $Cu(OH)_2$ precipitate and gradually grown on the substrates and wall of the container. Subsequent heating of the solution (Eq. (9)) causes this decomposition. From the XRD patterns of as-synthesized and annealed films it was concluded that the grown film completely composed of only CuO molecules.

## 4. Conclusion

In summary, we have synthesized dense and continuous CuO plate-like nanostructures by a simple, low temperature and cost effective solution method. SEM, XRD and dark resistivity investigations on the nanostructures have been carried out. From SEM analysis the RMS thicknesses of the nanostructures are found about 100 nm. XRD patterns showed that the synthesized structures have good crystallinity with monoclinic crystal structure preferentially in $(\bar{1}\,1\,1)$ and $(1\,1\,1)$ directions. From temperature dependant dark

electrical measurements the band gap energies of as-synthesized and annealed films at 300 °C for 1 h are found as 1.37 eV and 1.39 eV and the ionization energies the impurity levels of as-synthesized and annealed films at 300 °C for 1 h are found as 0.30 eV and 0.32 eV respectively. And all these values are in agreement with the literature.

## Acknowledgement

This work is financially supported by the Scientific Research Commission of Gaziosmanpaşa University (Project No: 2008/30).

## References

[1] S. Iijima, Nature 354 (1991) 56.
[2] M.Y. Yen, C.W. Chiu, C.H. Hsia, F.R. Chen, J.J. Kai, C.Y. Lee, H.T. Chiu, Adv. Mater. 15 (2003) 235.
[3] J.B. Chang, J.Z. Liu, P.X. Yan, L.F. Bai, Z.J. Yan, X.M. Yuan, Q. Yang, Mater. Lett. 60 (2006) 2125.
[4] J.T. Chen, F. Zhang, J. Wang, G.A. Zhang, B.B. Miao, X.Y. Fan, D. Yan, P.X. Yan, J. Alloys Compd. 454 (2008) 268.
[5] Z.W. Liu, Y. Bando, Adv. Mater. 15 (2003) 303.
[6] W. Wang, Z. Liu, Y. Liu, C. Xu, C. Zheng, G. Wang, Appl. Phys. A: Mater. 76 (2003) 417.
[7] X. Wen, W. Zhang, S. Yang, Z.R. Dai, Z.L. Wang, Nano. Lett. 2 (2002) 1397.
[8] Y. Chang, H.C. Zeng, Cryst. Growth Des. 4 (2004) 397.
[9] G.H. Yue, P.X. Yan, D. Yan, J.Z. Liu, D.M. Qu, Q. Yang, X.Y. Fan, J. Crystal Growth 293 (2006) 428.
[10] J.Q. Hu, Y. Bando, J.H. Zhan, Y.B. Li, T. Sekiguchi, Appl. Phys. Lett. 83 (2003) 4414.
[11] J.J. Wang, M.Y. Zhu, R.A. Outlaw, X. Zhao, D.M. Manos, B.C. Holloway, V.P. Mammana, Appl. Phys. Lett. 85 (2004) 1265.
[12] F. Favier, E.C. Walter, M.P. Zach, T. Benter, R.M. Penner, Science 293 (2001) 2227.
[13] W. Jia, E. Reitz, P. Shimpi, E.G. Rodriguez, P.X. Gao, Y. Lei, Mater. Res. Bull. 44 (2009) 1681.
[14] A.Y. Oral, E. Mensur, M.H. Aslan, E. Basaran, Mater. Chem. Phys. 83 (2004) 140.
[15] J. Yang, L.C. Jiang, W.D. Zhang, S. Gunasekaran, Talanta 82 (2010) 25.
[16] J. Zhu, D. Li, H. Chen, X. Yang, L. Lu, X. Wang, Mater. Lett. 58 (2004) 3324.
[17] Q. Liu, H. Liu, Y. Liang, Z. Xu, G. Yin, Mater. Res. Bull. 41 (2006) 697.
[18] V.R. Katti, A.K. Debnath, K.P. Muthe, Manmeet Kaur, A.K. Dua, Sens. Actuators B: Chem. 96 (2003) 245.
[19] Z. Yang, J. Xu, W. Zhang, A. Liu, S. Tang, J. Solid State Chem. 180 (2007) 1390.
[20] L. Cheng, M. Shao, D. Chen, Y. Zhang, Mater. Res. Bull. 45 (2010) 235.
[21] B. Li, Y. Wang, Superlattices Microstruct. 47 (2010) 615.
[22] S. Jana, S. Das, N.S. Das, K.K. Chattopadhyay, Mater. Res. Bull. 45 (2010) 693.
[23] J. Liu, X. Huang, Y. Li, Z. Li, Q. Chi, G. Li, Solid State Sci. 10 (2008) 1568.
[24] D.P. Dubal, D.S. Dhawale, R.R. Salunkhe, V.S. Jamdade, C.D. Lokhande, J. Alloy. Compd. 492 (2010) 26.
[25] Y. Xu, C. Wang, D. Chen, X. Jiao, Mater. Lett. 64 (2010) 249.
[26] V.R. Shinde, C.D. Lokhande, R.S. Mane, S.H. Han, Appl. Surf. Sci. 245 (2005) 407.
[27] S.M. Sze, Semiconductor Devices, Physics and Technology, Wiley, New York, 1985.
[28] K. Seeger, Semiconductor Physics, Springer, Berlin/Wien/New York, 1973.
[29] B. Pejova, A. Tanusevski, I. Grozdanov, J. Solid State Chem. 178 (2005) 1786.
[30] R.A. Zarate, F. Hevia, S. Fuentes, V.M. Fuenzalida, A. Zuniga, J. Solid State Chem. 180 (2007) 1464.
[31] G. Hodes, Chemical Solution Deposition of Semiconductor Films, Marcel Dekker, Inc., New York, 2002, 377 pp.